PHYSICAL REVIEW D **70**, 034506 (2004)

Estimate of the flavor singlet contributions to the hyperfine splitting in charmonium

C. McNeile* and C. Michael

(UKQCD Collaboration)

Theoretical Physics Division, Dept. of Mathematical Sciences, University of Liverpool, Liverpool L69 3BX, United Kingdom

(Received 17 February 2004; revised manuscript received 5 May 2004; published 17 August 2004)

We explore the splitting between flavor singlet and non-singlet mesons in charmonium using unquenched lattice QCD. The non-perturbatively improved clover formalism is used for both the sea and valence quarks. This has implications for lattice calculations of the hyperfine splitting in charmonium.

DOI: 10.1103/PhysRevD.70.034506 PACS number(s): 11.15.Ha, 12.38.Gc, 14.40.Cs

I. INTRODUCTION AND MOTIVATION

In the past year there have been many new interesting experimental discoveries in meson spectroscopy with heavy quarks [1]. One of the goals of the experimental program at CLEO-c [2] is to refine our experimental knowledge of the heavy hadron spectrum. This new data helps to validate methods, such as lattice gauge theory, that solve QCD non-perturbatively.

On the theoretical side, it has been claimed that there has been much progress in unquenched lattice QCD calculations [3]. These new lattice QCD calculations that use improved staggered quarks have passed some important experimental consistency checks [3]. However, the one place where the agreement between lattice QCD and experiment is still poor is the mass splitting between the J/ψ and η_c [4]. The masses of these two mesons can usually be computed with the smallest statistical errors. Also, as these masses are independent of light valence quarks, this splitting does not depend on a large extrapolation in the valence quark mass. It does of course depend on an extrapolation in the sea quark mass.

The experimental value for the mass splitting between the J/ψ and η_c is 116 MeV. Quenched lattice QCD calculation tend to significantly underestimate the hyperfine splitting in charmonium. Some of the older lattice calculations [5–13] that computed this splitting have been reviewed recently [14].

El-Khadra [6] originally argued that the hyperfine splitting in charmonium was very sensitive to ''unquenching.'' Lattice calculations after El-Khadra's [6] work essentially confirmed the original findings [14] (as well as providing information about new states). However, there is another technical complication. When using a clover improved fermion formalism on the lattice, the hyperfine splitting is sensitive to the coefficient c_{SW} (of a term in the fermion operator that helps reduce lattice spacing dependence on physical quantities) at nonzero lattice spacing, but the hyperfine splitting should be independent of the c_{SW} as the continuum limit is taken, because the clover term is an irrelevant operator. The value of c_{SW} can be computed in perturbation theory or via a non-perturbative numerical method. The high computational cost of reducing the lattice spacing in unquenched lattice QCD calculations may make it hard to disentangle the effects of getting a reduced hyperfine splitting due to unquenching effects and an imprecise value of c_{SW}. Recently the QCD-TARO Collaboration [15,16] have studied the charmonium spectrum in quenched QCD using the clover action at a smaller lattice spacing ($a^{-1} \sim 5$ GeV) than previously used. They obtained a hyperfine splitting of 77(2)(6) MeV in the continuum limit. They also verified that the hyperfine spitting in charmonium was independent of the value c_{SW} in the continuum limit.

There has not been much work on the charmonium spectrum from unquenched lattice QCD calculations. There are arguments based on potential models, that suggest the hyperfine splitting in charmonium is sensitive to the presence of light sea quarks [6,17]. It has been found that unquenched calculations are cheaper for staggered fermions than Wilson formulation, hence most previous calculations of the charmonium spectrum have used staggered sea quarks. Unfortunately, there are technical complications with using staggered fermions with masses as heavy as charm, so most groups use either clover, Wilson or NRQCD fermions for the charm quarks. El-Khadra *et al.* [18] did look at the charmonium spectrum on (unimproved) staggered gauge configurations [m_π/m_ρ was 0.6 and the lattice spacing was $a^{-1} \sim 0.99(4)$ GeV] from the MILC Collaboration. No significant increase in the hyperfine splitting was reported. Stewart and Koniuk [19] studied the charmonium spectrum using NRQCD on unquenched (unimproved) staggered gauge configurations ($m_\pi/m_\rho \sim 0.45$ and $a \sim 0.16$ fm). Any signal for the effect of unquenching was hidden beneath the systematic uncertainties in using the NRQCD formalism for charmonium.

The work by Davies *et al.* [3,20] found that the correct ratio was produced for the (P-S)/(2S-1S) mass splittings for $\overline{b}b$ using unquenched calculations with improved staggered fermions. However, the hyperfine splitting in charmonium is still incorrect [4,21,22] at 97 ± 2 MeV. The authors claim that the discrepancy may be caused by the clover coefficient only being used to tree level in tadpole improved perturbation theory. These calculations do, however, get the hyperfine splitting, the so-called J parameter [23], in the light quark sector correct [20].

There is another possible reason that the hyperfine mass splitting between the J/ψ and η_c is smaller than experiment

*Electronic address: mcneile@amtp.liv.ac.uk

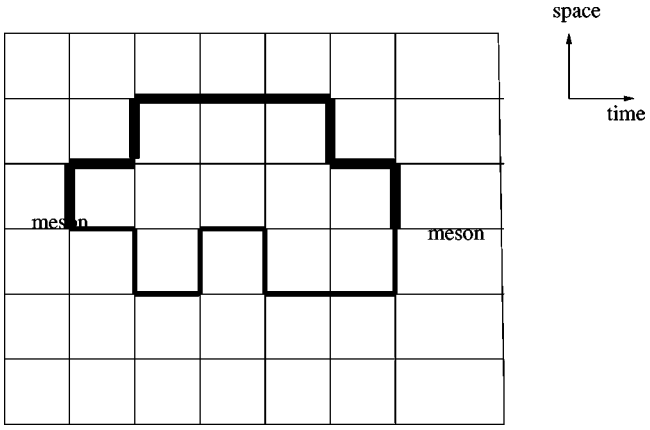

FIG. 1. Connected loop contribution to the propagator.

in current lattice evaluations. This has been also discussed recently by QCD-TARO [14–16,24]. All lattice calculations have computed the non-singlet correlator (see Fig. 1). However, charmonium interpolating operators are actually singlet $(\bar{c}\Gamma c)$, so the Wick contractions contain bubble diagrams (see Fig. 2). The bubble diagrams are OZI suppressed so should be small. However, this argument will fail if there is additional non-perturbative physics. For light mesons [25], it has been found that the effects of the bubbles can be large for the pseudoscalar and scalar mesons where the additional physics is the anomaly and the 0^{++} glueball, respectively, but not for other channels. Essentially, the disconnected loops are large if there is additional interesting physics such as glueballs, the anomaly, or instantons. It is possible to explore this non-perturbatively from the lattice and we discuss these mechanisms in Sec. VI.

It is interesting to compare the hyperfine splitting for D mesons with that in charmonium, as there is no contribution from the bubble diagrams for the D mesons. In Table I we have collected some results for the $D^\star - D$ mass splitting from quenched QCD. The agreement between experiment and lattice is pretty good for the mass splitting between the $D^\star$ and D. The differences could be explained by the ambiguity in determining the lattice spacing in quenched QCD. As noted recently by di Pierro *et al.* [21], the hyperfine splitting in the D system is first order in the clover coefficient,

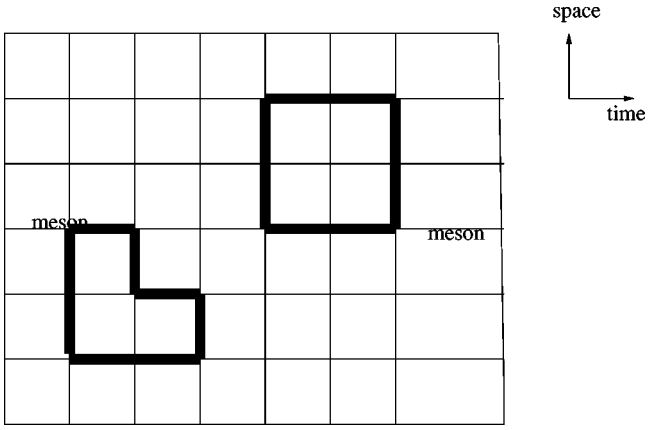

FIG. 2. Disconnected loop contribution to the propagator.

TABLE I. Collection of hyperfine splittings between the D and $D^\star$ mesons.

Group	Method	$M_{D^\star} - M_D$ MeV
Boyle [26]	clover	124(8)(15)
Boyle [27]	$\beta = 6.0$ tadpole clover	106(8)
Hein *et al.* [28]	NRQCD $\beta = 5.7$	$110^{+3+22}_{-0-0}(3)(6)(5)$
UKQCD [29]	NP clover $\beta = 6.2$	130^{+6+15}_{-6-35}
UKQCD [30]	NP clover $\beta = 6.2$	127(14)(1)(3)
PDG [31]	Experiment	142.12(7)

but the hyperfine splitting in charmonium is second order in the clover coefficient. Hence, the hyperfine splitting in charmonium may be more sensitive to the clover coefficient. The differences in the hyperfine splitting may potentially be due to remaining errors in the determination of c_{SW}.

It is clearly not sufficient to just assume that the OZI-violating disconnected contributions to charmonium states are negligible, particularly as they are responsible for the decay width of η_c of some tens of MeV. In order to clarify these issues, we explore from first principles the importance of disconnected contributions to the charmonium hyperfine splitting, using unquenched lattice calculations that use the non-perturbatively improved clover formulation.

In this paper we first discuss in Sec. II the formalism for computing the mass splitting between the singlet and non-singlet mesons. We then report our results for the masses of the non-singlet mesons in charmonium in Sec. IV. We next discuss our results for singlet mesons in Sec. V. In the final Sec. VI, we put our numerical results on the contribution of the singlet correlator to the charmonium masses in context with a discussion about the phenomenology of OZI effects and decay widths in the charmonium system.

II. SINGLET CORRELATORS

In lattice studies it is possible to measure separately the non-singlet contribution given by connected correlation $C(t)$ (see Fig. 1) and the flavor singlet contribution which has an additional disconnected correlation $D(t)$ (see Fig. 2). Previous lattice studies have been made of the light pseudoscalar mesons [32–36] and scalar mesons [37–41]. For a discussion including some results for vector and axial mesons, see [42].

In the flavor singlet case there is an additional disconnected correlation $D(t)$ to be evaluated. This correlation can be written in the form

$$D(t) = N_f r_4 r_5 \langle L(0) L^*(t) \rangle \tag{1}$$

where the disconnected loop

$$L(t) = \mathrm{Tr}\, \Gamma M^{-1} \tag{2}$$

with M^{-1} the quark propagator and the sum in the trace is over color, Dirac and spatial indices at time t. We discuss values for number of flavors (N_f) later on in this section. Here we assume that the hadron under consideration is cre-

ated by $\bar{q}\Gamma q$ and so the factor of r_4 arises from reflection positivity (i.e., $\gamma_4\Gamma^\dagger = r_4\Gamma\gamma_4$). The factor of r_5 arises since the Wilson-Dirac fermion matrix M is γ_5 Hermitian and hence L is real/imaginary as $\gamma_5\Gamma = r_5\Gamma\gamma_5$ with $r_5 = \pm 1$. Since at $t=0$ we have that $L(0)L^*(0) > 0$, the disconnected correlation $D(0)$ has sign $r_4 r_5$.

At large t where ground state contributions dominate we have

$$C(t) = ce^{-m_1 t} \tag{3}$$

and

$$C(t) + D(t) = de^{-m_0 t} \tag{4}$$

where m_0 is the flavor singlet mass and m_1 the flavor non-singlet mass. Here we are ignoring lighter singlet pseudoscalar states (with no charm content, such as η) which contribute with very small amplitude to $C+D$. If the same meson creation and destruction operators are used for the study of both correlations, with quarks degenerate in mass, d and c have the same sign.

Then by a study of D/C which is given by

$$D(t)/C(t) = (d/c)e^{(m_1 - m_0)t} - 1 \tag{5}$$

the mass splitting between flavor singlet and non-singlet can be explored. Although it might be thought that $d=c$, we have shown previously [40] that this is not necessarily the case, and indeed sign changes in D/C versus t can be required. So, in summary, the slope (increase/decrease) of D/C on a lattice can determine the sign and magnitude of $m_1 - m_0$. For charmonium it is correct to use $N_f = 1$ in Eq. (1) since only one flavor of quark can contribute to the loops. In our comparisons using lighter quarks for the loops, we will also use $N_f = 1$. We have previously published results for the masses of the light scalar singlet [41] and light singlet pseudoscalar mesons [43] from this data set.

Since, as we shall see, the disconnected contributions are poorly determined as t increases, it is advantageous to remove excited state contributions as far as possible. One technique, pioneered by Neff *et al.* [44], is to study the ratio of D/C using the ground state contribution to the connected correlator C from a fit. This will be appropriate if the disconnected contribution D has only small excited state contributions, as does seem to be the case:

$$D(t)/C(t)_{fit} = (d/c)e^{(m_1 - m_0)t} - 1. \tag{6}$$

The results from applying this formalism are discussed in Sec. V B.

III. LATTICE METHODOLOGY

We use dynamical fermion configurations with $N_f = 2$ from UKQCD [45]. The sea quarks correspond to $\kappa = 0.135$ with a non-perturbative improved clover formalism. The volume was $16^3 32$. This data set has a scale set by [45] $r_0/a = 4.754(40)(+2-90)$ and pseudoscalar meson to vector meson mass ratio of $m_P/m_V = 0.70$. Using the value $r_0 = 0.525$ fm then gives $a^{-1} = 1790$ MeV while the meson mass ratio implies that the sea quarks have masses close to that of a strange quark. We have already reported the spectrum of the charm-strange mesons and preliminary results for the mass of the charm quark on this data set [46,47].

Local and spatially-fuzzed operators [48] are used for meson creation (with two fuzzed links in a spatially symmetric orientation with 5 iterations of fuzzing with coefficient given by 2.5*Straight + Sum of staples). Thus we evaluate a 2×2 matrix of local and fuzzed correlators [48]. Mesons created by all independent products of gamma matrices are evaluated.

We measured the connected and disconnected correlations on 201 configurations of size $16^3 32$ separated by 40 trajectories for three heavy κ values: 0.113, 0.119, 0.125. This data set was used to estimate the κ value for the mass of the charm quark. Our preliminary estimate for the κ value at the charm quark mass was close to 0.119. As the aim of this study was to look for the singlet contribution to the charmonium correlators, we did additional runs at $\kappa = 0.119$. At $\kappa = 0.119$, we computed connected and disconnected correlators separated by 10 sweeps, hence the ensemble size was 788. The correlators were then blocked with a block size of 40 sweeps. At $\kappa = 0.119$, all the results reported here are from the higher statistics run.

For the evaluation of the disconnected correlators, we use 100 stochastic noise sources with the two source trick described in [40]. We use sources at every site on the lattice and determine the momentum-zero correlations from them. The connected correlators are obtained by explicit inversion from a source (local or fuzzed) [45].

IV. ANALYSIS OF THE CONNECTED CORRELATORS

The lattice spacing used in this data set is large relative to the mass of the charm quark, hence lattice spacing errors are a potential concern. In quenched QCD it is computationally possible to use finer lattice spacings, so lattice spacing errors can be controlled by ''brute force'' [15,16]. The high cost of reducing the lattice spacing in unquenched calculations means that a brute force approach will not be feasible for many years with this type of fermion action. Hence we chose to investigate the heavy quark formalism developed by the Fermilab group [49].

The lattice artifacts modify the dispersion [49,50] relation:

$$E^2 = M_1^2 + \frac{M_1}{M_2}p^2 + O(p^4) \tag{7}$$

where M_1 is known as the ''rest mass'' and M_2 is the kinetic mass [since $E = M_1 + p^2/(2M_2) + O(p^4)$]. In the FNAL lattice heavy quark formalism [49], the rest mass is affected by lattice artifacts, but the M_2 mass is the one that controls the dynamics of the states. The quality of the disconnected data precluded us obtaining any useful information from the disconnected data with non-zero momentum. A definition of the kinetic mass (M_2) in terms of the energy E of the meson is:

$$\frac{1}{M_2} = 2\frac{\partial E}{\partial p^2}|_{p=0}. \tag{8}$$

There are a number of different ways to define the quark masses on the lattice. For Wilson and Clover fermions, the vector definition of the quark mass is

$$m_v = \frac{1}{2}\left(\frac{1}{\kappa} - \frac{1}{\kappa_{crit}}\right) \tag{9}$$

where κ_{crit} is the value of κ where the pion mass vanishes. In tree level perturbation theory [49], the kinetic definition of the quark mass m_2 is related to the vector definition of the quark mass (m_v).

$$m_1 = \ln(1+m_v) \tag{10}$$

$$\frac{1}{m_2} = \frac{2}{m_v(2+m_v)} + \frac{1}{1+m_v}. \tag{11}$$

In the ALPHA formulation [51] the vector definition of the quark mass is O(a) improved using

$$\hat{m}_v = m_v(1+b_m m_v) \tag{12}$$

where the value of b_m from perturbation theory is

$$b_m = -\tfrac{1}{2} - 0.0962g^2. \tag{13}$$

There are different ways of including the b_m term in the calculations. The merits of the different ways are discussed in the UKQCD paper [29] on heavy-light decay constants. The tadpole improved expressions for the FNAL quark masses are obtained by replacing m_v with m_v/u_0, where $u_0 = 1/(8\kappa_{crit})$.

To find the value of κ for the charm quark, we interpolate the spin averaged heavy meson mass

TABLE II. Results for the masses from the fits to the connected data at $\kappa = 0.119$. The masses of the ground and first excited state (denoted by 2S or 2P) are shown. The M_1 and M_2 masses are the meson masses from the Fermilab formalism [from Eq. (7)]. The fit regions and χ^2/DOF are from the momentum zero fits.

Particle	region	χ^2/DOF	aM_1	aM_2	$\frac{M_1}{M_2}$
0^{-+}	3 - 13	2.7/24	1.549(1)	2.01(2)	0.772(8)
0^{-+}(2S)	3 - 13	2.7/24	2.02(3)	1.6(2)	1.3(2)
1^{--}	3 - 13	2.3/24	1.593(2)	2.06(2)	0.772(8)
1^{--}(2S)	3 - 13	2.3/24	2.09(3)	1.6(2)	1.3(2)
0^{++}	3 - 14	20/27	1.790(6)	2.5(2)	0.71(5)
0^{++}(2P)	3 - 14	20/27	2.38(5)	-	-
1^{+-}	3 - 13	8.8/24	1.805(9)	-	-
1^{+-}(2P)	3 - 13	8.8/24	2.31(5)	-	-
1^{++}	3 - 13	16.4/24	1.816(7)	-	-
1^{++}(2P)	3 - 13	16.4/24	2.39(5)	-	-

$$M_{Sav} = \tfrac{1}{4}(3M_V + M_{PS}) \tag{14}$$

linearly with the vector definition of the quark mass to the experimental value at 3068 MeV. For the data set with correlators separated by 40 sweeps, we fitted a two exponential factorizing fit model to the 2 by 2 smearing matrix. From that, using M_1, we obtain the kappa value of 0.116 for the charm quark. We comment later on the consequences of using other definitions of the mass.

We used ''factorizing fits'' with three exponentials to fit the two by two matrix of smeared correlators for the higher statistics data set. The results for the ground and first excited masses are in Table II for both the M_1 and M_2 definitions of the meson masses in the Fermilab formalism. The effective mass plots, corresponding to a subset of the data in Table II, for the pseudoscalar (0^{-+}) and scalar channels (0^{++}) are in Figs. 3 and 4.

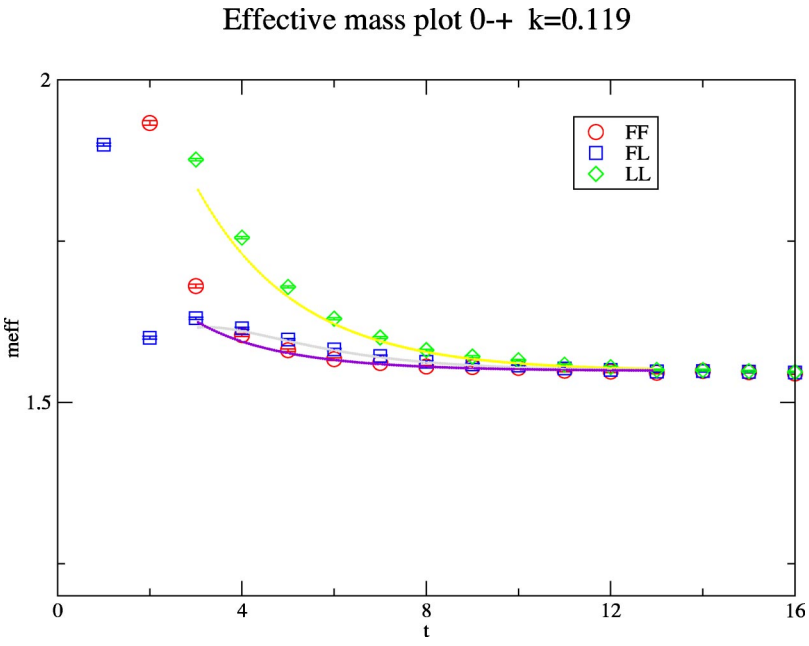

FIG. 3. Effective mass plots for the fuzzed-fuzzed (FF), fuzzed-local (FL), and local-local (LL) correlators for the pseudoscalar at $\kappa = 0.119$. The fitted correlators are also shown.

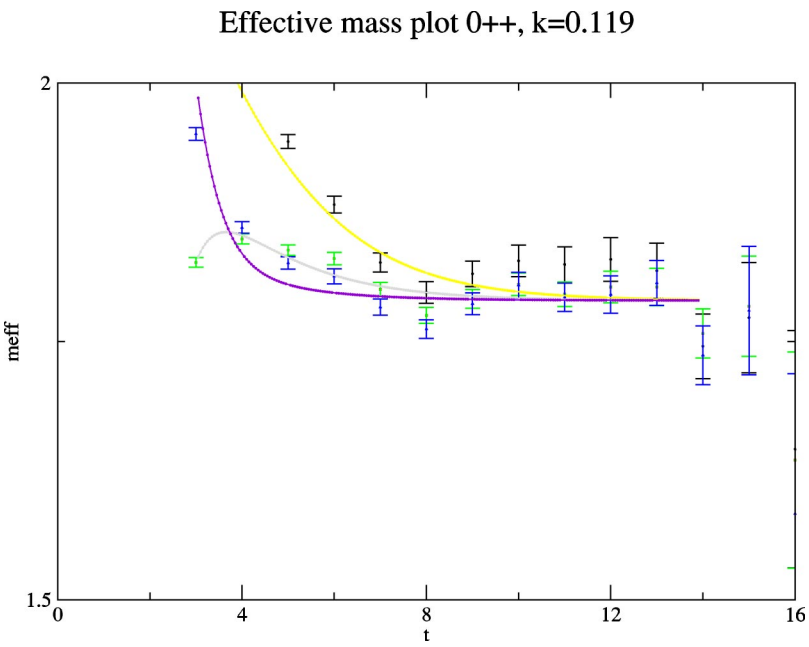

FIG. 4. Effective mass plot for the 0^{++} state at $\kappa=0.119$. The notation is the same as for Fig. 3.

The dispersion relation of the heavy-heavy pseudoscalar channel is plotted in Fig. 5. At the lattice spacing for this calculation, the kinetic and rest masses differ by a significant amount. In Fig. 6 we plot the various definitions of the meson mass as a function of the quark mass [defined from the vector Ward identity, Eq. (9)]. In quenched QCD at finer lattice spacings (0.07 fm) UKQCD [29] has shown that the M_1 and M_2 masses essentially agree. The high computational cost of reducing the lattice spacing forces us to remain in a region where M_1 and M_2 still differ and we determine both masses. We fit Eq. (7) to the dispersion relation to calculate the M_2 mass.

The correlators with non-zero momentum are noisier than those with zero momentum. There are perturbative expressions for the kinetic meson mass in terms of the rest mass of the meson mass. At tree level [50]

$$M_2^{PT}=M_1+(m_2-m_1). \tag{15}$$

Our results for the M_1, M_2, and M_2^{PT} are plotted against the vector definition of the quark mass in Fig. 6. The tree level perturbative expression does not fit the numerical data very well.

Table III contains the mass splittings of the non-singlet P-wave mesons relative to the spin averaged S-wave meson mass [Eq. (14)], computed using the data in the Table II. The errors were computed using the bootstrap method.

The results for the M_2 mass for the excited states are very peculiar: we do see a linear behavior of E^2 versus p^2 so that M_2 can be extracted, but for the excited states it is *smaller* than for the ground state. This illustrates the limitation of interpreting M_2 as the meson mass and implies that a more sophisticated treatment is needed to deal with heavy quarks [52]. The JLQCD Collaboration also argue that the kinetic mass is not necessarily superior to the pole mass [52,53].

There is a lot of experimental interest in the mass of the $\eta_c(2S)$ meson [54]. Until recently the mass of the $\eta_c(2S)$

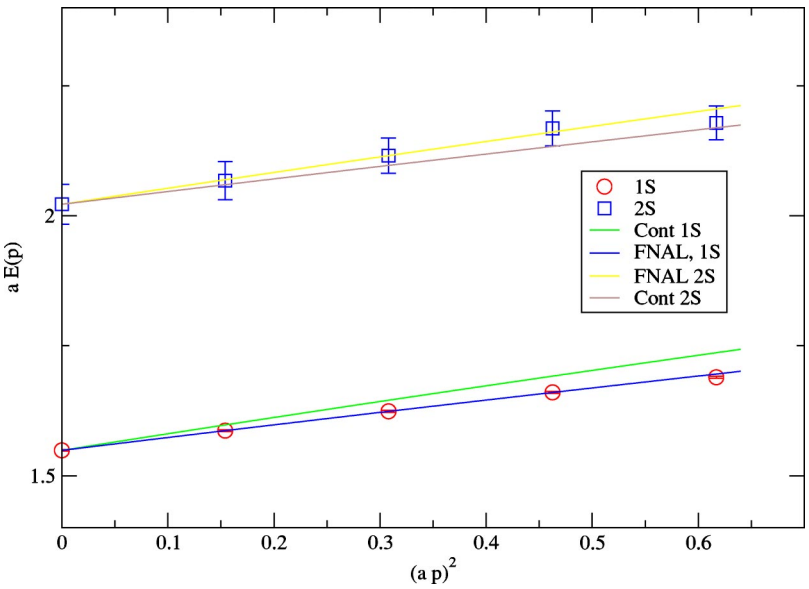

FIG. 5. Dispersion relation for the pseudoscalar at $\kappa=0.119$. The FNAL curve is for Eq. (7) and the Cont curve is the continuum dispersion relation [Eq. (7) with $M_1=M_2$].

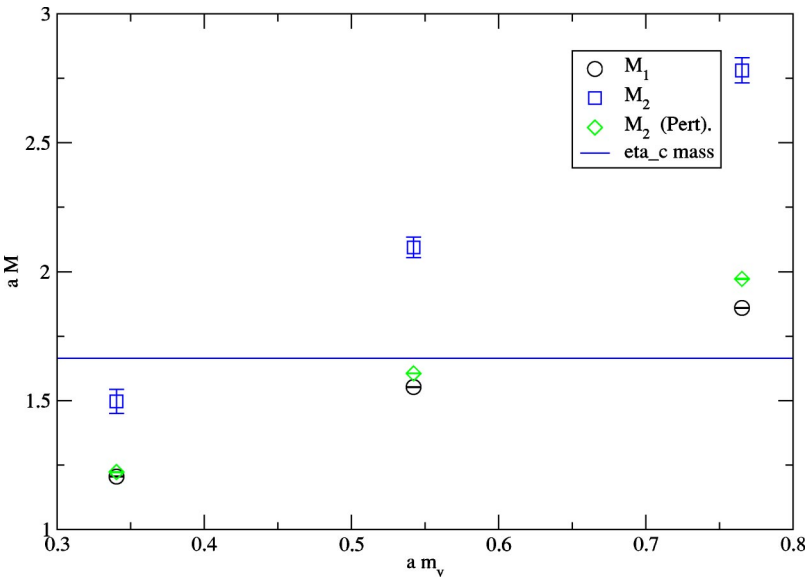

FIG. 6. Different definitions of the pseudoscalar meson mass versus the vector quark mass, in lattice units. This shows that the central quark mass value (from $\kappa=0.119$) is close to the experimental mass using M_1. The perturbative expressions are from Eq. (15).

determined from the Crystal Ball Collaboration [55] was larger than the predictions from potential models [56]. However, the new results for the mass of the $\eta_c(2S)$ from CLEO, BABAR, and BELLE are in much better agreement with potential models [54]. In Table IV we collect the results from some quenched lattice calculations and some recent experiments. Our result for the first excited hyperfine splittings is probably effected by lattice spacing errors. We discuss the effect of glueballs on the $\eta_c(2S)$ meson in Sec. VI.

V. ANALYSIS OF THE DISCONNECTED CORRELATORS

A. Stochastic noise compared to signal

We measure the zero momentum disconnected loop $L(t)$ on each time-slice for each gauge configuration. This ensemble, for each choice of operator Γ gives us the values of the standard deviation $\sigma_{\rm obs}$ given in Table V. We also, from our 100 stochastic samples in each case, have the estimate of the standard deviation $\sigma_{\rm stoch}$ on the mean of these 100 samples coming from the stochastic method. We can then deduce the true standard deviation of the gauge time slices from $\sigma_{\rm gauge}=(\sigma^2_{\rm obs}-\sigma^2_{\rm stoch})^{1/2}$. This is presented in Table V. Here the normalization is such that $M=1+\kappa\ldots$.

In an ideal world we would have $\sigma_{\rm stoch}\ll\sigma_{\rm gauge}$ which would imply that no appreciable error arose from the stochastic methods employed. The signal in the vector channel is dominated by the stochastic error. So for that case, either many more samples are required or an improved algorithm, such as variance reduction [40,60]. For the other cases, the stochastic noise is smaller than the intrinsic gauge fluctuation, and so more stochastic samples would not improve the results significantly.

From Table V the error on the heavy-heavy data is much less than that from the light-light data. This is a consequence of increased diagonal dominance of the fermion operator as the mass of the quark is increased. This is the basis of improved variance methods [40,60,61].

B. Results

We present in Figs. 7 and 8 some of our results for the ratio of the disconnected correlator to the connected correlator for the heavy kappa value and light kappa value, respectively. We also measured with fuzzed operators for the disconnected diagrams, but they are more noisy than the local operators we present here.

The error on the disconnected correlator is much larger than that on the connected one. This arises essentially because the absolute error on the disconnected correlator stays of the same magnitude as t increases, much as is the case for correlations between Wilson loops as used in glueball studies. The connected correlator, in contrast, has an approximately constant relative error as t increases. We are forced to consider the ratio of disconnected to connected correlator at rather low t-values because of the increasing errors on the disconnected correlator.

For light (close to the strange quark mass) disconnected contributions we find similar results in Fig. 8 to those ob-

TABLE III. Mass splittings from this data set using the data from Table II with a bootstrap error analysis. S_{av} is the spin averaged mass [see Eq. (14)]. The experimental numbers come from the Particle Data Group.

Splitting	a ΔM_1	ΔM_1 MeV	a ΔM_2	ΔM_2 MeV	Expt. MeV
$1^{--}-0^{-+}$	0.0446(6)	80(1)	0.06(1)	105(19)	116
$1^{--}(2S)-0^{-+}(2S)$	0.07(1)	126(24)	−0.01(10)	−18(189)	32
$0^{++}-S_{av}$	0.207(6)	371(11)	0.5(2)	864(330)	348
$0^{-+}(2S)-S_{av}$	0.44(3)	787(59)	-	-	587

TABLE IV. Collection of results for the excited hyperfine splittings between the $\psi(2S)$ and $\eta_c(2S)$ from lattice QCD and experiment.

Group	Method	$M_{\psi(2S)}-M_{\eta_c(2S)}$ MeV
Columbia [12]	anisotropic, lattice	75(44)
CP-PACS [13]	anisotropic, lattice	26(17)
PDG [31]/Belle [57]	Particle data table	$32\pm6\pm8$
CLEO [58]	Experiment	$43\pm4\pm4$
BABAR [59]	Experiment	55 ± 4
Crystal Ball [55]	Experiment	92 ± 5

tained from the lattice previously [25], namely very little signal for vector mesons but a large signal for pseudoscalar mesons that will increase the singlet mass over the non-singlet.

For charm quarks, we present our results in Figs. 7 and 9. There is only a statistically significant signal at small time values, so no definitive statement can be made. For the pseudoscalar, the slope for non-zero t is positive which corresponds to a reduction in the singlet mass compared to the non-singlet. We show on the figure lines corresponding to a mass shift of 18 and 36 MeV. This indicates that we cannot rule out a downward shift of the η_c mass by as much as 36 MeV. For the vector case, the signal is smaller (in Fig. 7) and shows no sign of a significant slope.

As we discuss below, we expect the splittings in the vector channel to be small and our results at $t\neq 0$ are consistent with that. We do find room, however, for splittings of the order of 20 MeV, particularly for the pseudoscalar channel. We have shown that the contribution of the singlet correlators to the hyperfine splitting in charmonium may be significant. From this calculation, it seems reasonable that the singlet correlators could contribute as much as 20 MeV to the hyperfine splitting. A more definitive estimate requires more uncorrelated gauge configurations and/or improved lattice formulations.

VI. DISCUSSION

We first recall our previous results from studying the light singlet mesons [25] on a lattice. The splitting in mass of flavor singlet and non-singlet mesons with the same quark content arises from gluonic interactions. The assumption that these are small is known as the OZI rule. For the pseudoscalar mesons this splitting is not small (it is related to the η, η' mass difference), basically because of the impact of the anomaly. For scalar mesons the splitting is also expected to be large because of mixing with the nearby scalar glueball. It is usually assumed that the OZI rule is in good shape for the vector and axial mesons and we found small contributions only.

TABLE V. Mesons produced by different operators $\bar{\psi}\Gamma\psi$. The standard deviation of the loop operator of Eq. (2) is presented. Here σ_{stoch} is the error estimated from the 100 stochastic samples used and this is the used to deconvolute the observed spread to give the true standard deviation of the loop (σ_{gauge}).

κ	Γ	J^{PC}	σ_{obs}	σ_{stoch}	σ_{gauge}
0.135	γ_5	0^{-+}	33.6	13.91	30.6
0.135	γ_k	1^{--}	14.7	14.45	2.7
0.135	I	0^{++}	53.0	15.0	50.8
0.119	γ_5	0^{-+}	15.9	8.3	13.6
0.119	γ_k	1^{--}	9.1	9.003	1.2
0.119	I	0^{++}	23.6	10.9	20.9

The picture from the light singlet mesons is that the contribution of the disconnected piece to the correlators is small unless there is additional interesting dynamics. In the charmonium system one possible source of the interesting dynamics is glueballs. The simplest model is of a flavor singlet state obtained from the mixing of the flavor non-singlet state with a glueball, which causes the states to repel in energy, often called an avoided level crossing. We would expect this mixing to be strongest when a glueball lay near in energy to the charmonium state and we now discuss this.

Morningstar and Peardon [62] have computed the excited glueball spectrum in quenched QCD. They obtained masses of 2590(40)(130) MeV and 3640(60)(180) MeV for the ground and first excited states of the 0^{-+} glueball, respectively. Morningstar and Peardon computed the mass of the 1^{--} glueball to be 3850(50)(190) MeV. So it is not inconceivable that the η_c mass (2980 MeV) is effected more by glueball states than the J/ψ state. In Fig. 10 we plot the masses of the glueballs from quenched QCD versus the experimental numbers. With these glueball masses, the mixing model predicts that the singlet contribution to the η_c will increase the mass, but that the singlet contribution to J/ψ will decrease the mass. This would not help to resolve the discrepancy of the charmonium hyperfine splitting from non-singlet lattice studies. Moreover this glueball mixing model gives the opposite sign to the pseudoscalar mass shift than that indicated by our lattice determination of the disconnected contribution. Bali has also recently reviewed the influence of glueball states on the charmonium spectrum [24].

The hyperfine splitting between $\eta_c(2S)$ and $\psi(2S)$ states will also be interesting as it may be affected by the glueball states. The closeness of the glueball state to the $\psi(2S)$ state has been noticed by model builders [63]. The model for hadron decays for vector charmonium states involves the emission of three gluons. This model predicts that the branching ratio for $\psi(2S)\rightarrow\rho\pi$ is much larger than experiment. Attempts have been made to use the vector glueball and $\psi(2S)$

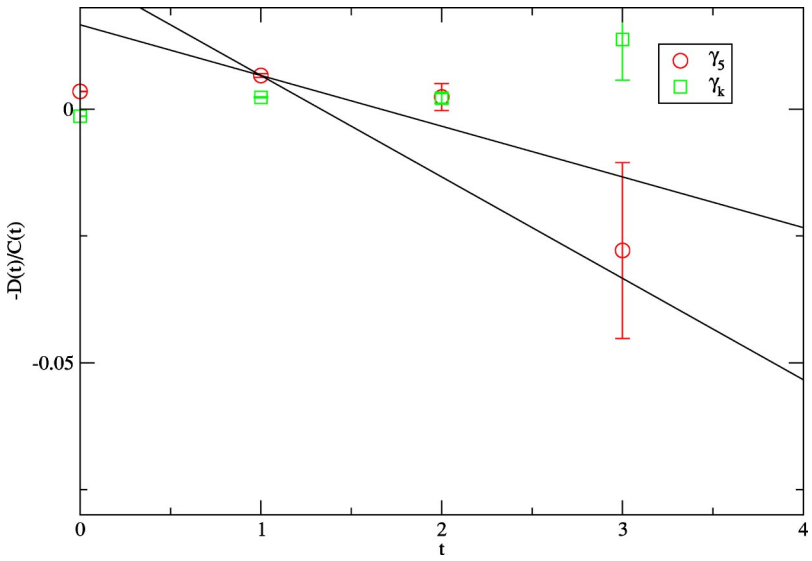

FIG. 7. The ratio of disconnected to connected contributions as given by Eq. (5) at the heavy κ value of 0.119. The straight lines with slopes of 0.01 and 0.02 (corresponding to a singlet mass 18 and 36 MeV, respectively, lighter than the non-singlet in physical units) are drawn to guide the eye.

mixing to account for this. If the glueball states have large widths, however, then it is unclear what the effect of the states will be on the charmonium spectrum.

As well as mixing with glueballs, there are other theoretical models which may give guidance on favor singlet mass splittings. Isgur and Thacker discuss the origin of the OZI rule from a quark model and the large N_c limit of QCD [42]. Schafer and Shuryak discuss the OZI rule using instanton-based methods [64].

Another approach is to relate the mass splitting to the fact that the decay products (or strongly coupled many-body channels) of the singlet and non-singlet state are different. One idea is that a mass shift can arise from the energy dependence of the decay width and will be more significant for wider resonances. It will also be possible that mass shifts can arise from the back-reaction of the decay channels to the effective propagator. One consequence of this, as has been known for a very long time [65], is that the pole in the complex plane corresponding to a resonance has an energy whose real part is lower than the quoted value which corresponds to a phase shift of 90°. This effect of hadron decay on the mass is also an issue for quark model calculations. Isgur and Geiger [66,67] discuss the effect of decay thresholds on the masses obtained from quark model calculations. In principle, the effect of hadronic decays can be introduced into quark models using coupled channel techniques [68]. However, it is difficult to write down a reasonable operator for pair creation.

This issue of the effect of coupled channels (including open decays) to the mass of a state is one that can be illuminated from lattice gauge theory. This is especially so for singlet states, since the lattice enables one to determine the relative contributions from the connected and disconnected diagrams separately.

In the quenched approximation, decays are not treated correctly. This can be a serious problem: the connected correlators include only part of the allowed two-body intermediate states and hence anomalous results can be obtained, as for the scalar meson [69]. Here we are using a dynamical quark formalism which is explicitly unitary (at least in a

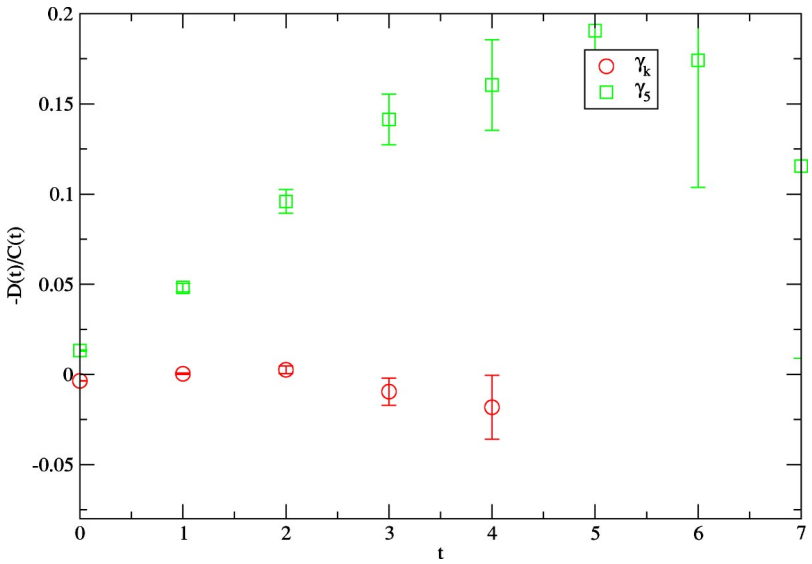

FIG. 8. The ratio of disconnected to connected contributions as given by Eq. (5) at the light κ value of 0.135.

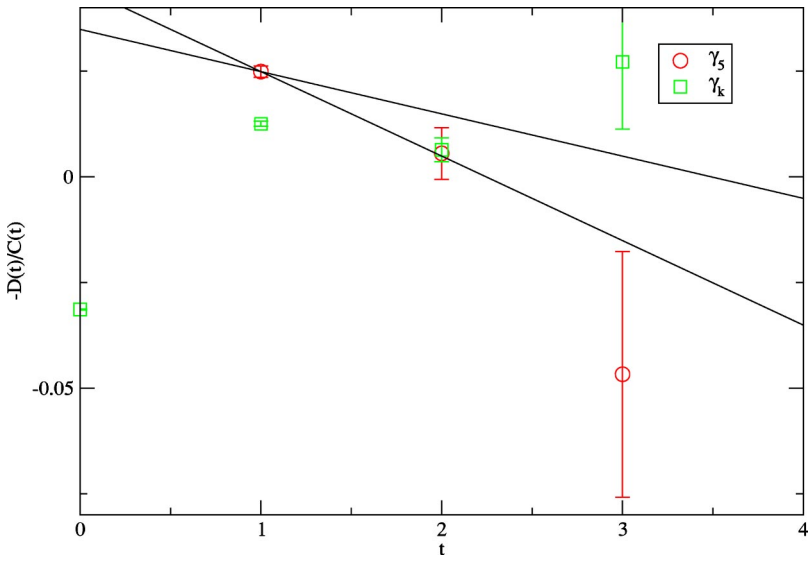

FIG. 9. The ratio of disconnected to connected contributions as given by Eq. (6) at the heavy κ value of 0.119. The SESAM method is used. The straight lines with slopes of 0.01 and 0.02 (18 and 36 MeV in physical units) are drawn to guide the eye.

world with only $N_f=2$ flavors of quark degenerate in mass). Within this formalism we can add charm quarks without expecting any significant breakdown of unitarity from neglected charm quark loops in the vacuum. Then the correct treatment of charmonium states is to add the connected and disconnected contributions, as we have emphasized. The connected diagram, once one remembers that light quark loops are present in the vacuum, contains intermediate states such as $D\overline{D}$ and $D^*\overline{D}$, etc. It does not contain charmless intermediate states. The hadronic decays of those charmonium states below the DD threshold are necessarily to charmless intermediate states. These are just the charmless states that are allowed as intermediate states in the disconnected diagram evaluated on the lattice. Thus there is a link between the disconnected diagram and the hadronic decay of the charmonium state. For an OZI-violating decay, the charm quark and anti-quark must annihilate which is similar process to the contribution of the disconnected diagrams (Fig. 2) to the singlet correlator. This link is not unambiguous for light quarks: for example the substantial η-π splitting (in a world with $N_f=2$) arises from the disconnected diagram but no hadronic decay of the η is allowed energetically. There does not seem to be a simple quantitative link between the mass shift caused by the disconnected loop in the correlator and the width of the state.

This link is explicit in a perturbative treatment of charmonium (even more so for $\overline{bb}$): one can evaluate the OZI violating contributions to charmonium from multiple gluon exchange. The pseudoscalar meson allows two gluon exchange and so should have much larger effects than for the vector meson where three gluons are needed. Moreover the hadronic decays are to multi-light-quark states created from these two (or three) gluon intermediate states.

The computation of strong decay widths from lattice QCD is a hard problem. There are formalisms available, but the numerical calculations are quite difficult. Some of the issues

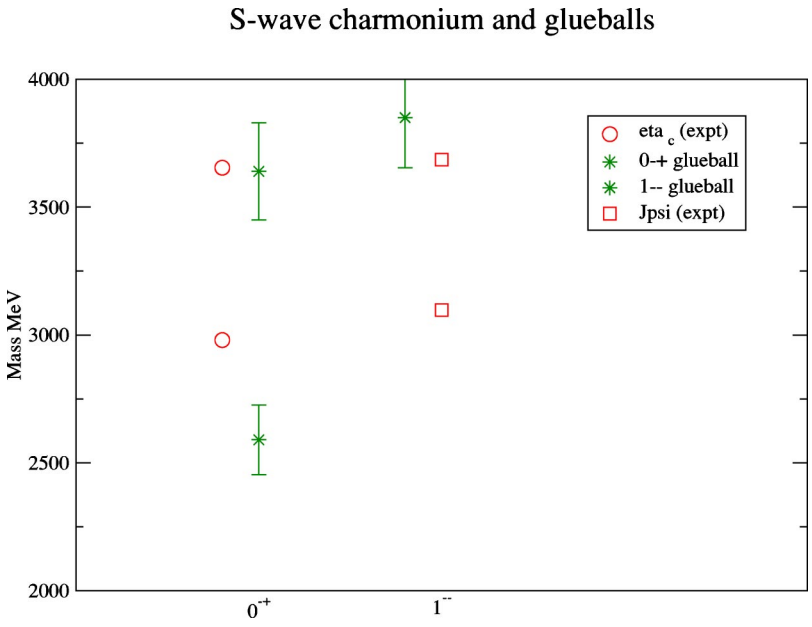

FIG. 10. Masses of the experimental pseudoscalar and vector states in charmonium with the glueball masses from quenched QCD.

about decay widths and lattice QCD have been recently been reviewed [70,71]. In a large lattice spatial volume, the effect of coupled two-body decay channels on the mass of a state is already taken account of by the formulation, provided one uses a unitary theory with the same valence quarks as sea quarks. Thus one should not expect any shift from decay channels. One example of this is that the baryon decuplet shows experimentally an equal mass spacing arising from the number of strange quarks present, even though the widths of the members vary from 120 MeV (Δ) to stable (Ω).

On a lattice, at smaller volumes, the two-body momentum states become discrete and this induces small shifts in mass. These have been exploited by Lüscher to yield information about two-body scattering from the lattice. An example of a shift in the ρ mass on a lattice from its coupling to $\pi\pi$ has also been studied [72].

For hadrons containing only light quarks it is difficult to compute decay widths from first principles on a lattice. For charmonium, decay widths can in principle be computed using the NRQCD factorization formalism [73,74], or from older techniques based on factorizing the decay width into a perturbative part and the wave function at the origin [75].

Thus we should interpret our results, for the mass splitting between the singlet and non-singlet mesons, as giving an indication of the strength and sign of OZI violating contributions to the heavy meson spectrum. These need not correspond to those observed experimentally because we would need to extrapolate our lattice results to the continuum limit and to more realistic quark masses (including a third flavor). This extrapolation in quark mass could be quite delicate, because of issues such as mixing and decays, as discussed above. We note that $\overline{bc}$ mesons will not have these singlet contributions and so the hyperfine splitting for them should agree with a lattice calculation using only connected contributions. This may be a useful experimental source of input into the composition of such states.

Both the η_c and J/ψ are below the threshold for $D\overline{D}$ decays. However OZI-violating hadronic decays are allowed. The current summary of the η_c properties in the particle data table [31], quotes the width of the η_c as $16^{+3.8}_{-2.1}$ MeV. However, the latest results for the width of the η_c are larger than the number in the Particle Data table. CLEO [76], BES [77], and BaBar [78] obtain for the η_c width: $27\pm5.8\pm1.4$ MeV, and $17\pm3.7\pm7.4$ MeV, and 33 ± 2.5 MeV, respectively. CLEO [76] note that a larger width ($\sim$28 MeV) for η_c improves agreement with experiment for the next to leading order perturbative QCD expressions [75] for the ratio of the decay width to the two photon width (which is more precisely known). This agreement with perturbative estimates also suggests that mixing with glueballs is not the dominant mechanism for the η_c decay, and hence for the η_c mass contribution from disconnected diagrams. We note that an η_c width of 30 MeV is comparable to the width of some $\overline{cc}$ mesons above the $\overline{DD}$ threshold, such as the $\psi(3770)$ with a width of 24 MeV, although typically the widths of $\overline{cc}$ mesons above threshold are above 80 MeV.

The width of the J/ψ is accurately known and is 87 keV [31]. The reason for the smaller width of the vector mesons is that the leading order perturbative corrections are $O(\alpha_s^3)$ for the vector channel, but $O(\alpha_s^2)$ for the pseudoscalar channel [75].

Although a width of 30 MeV is small relative to the mass of the η_c, this width is not small relative to the hyperfine splitting. It is the mass splittings that are the significant quantities in charmonium. So it is not unreasonable that there is a shift coming from OZI-violating intermediate states in the mass of the η_c of the order of 20 MeV and that the mass of the J/ψ is unaffected. This can be substantiated by more accurate lattice evaluations, our calculation leaves room for an effect of such a magnitude but with large errors.

It is claimed [3] that lattice calculations using improved staggered sea quarks, can compute certain quantities from continuum QCD to the few percent accuracy level. We feel that we have demonstrated, from both our lattice data and physical arguments, that the singlet contribution will have to be computed to get the hyperfine splitting in charmonium correct to this accuracy. Studies with anisotropic lattices may be useful to sample more intermediate points, but a long reach in physical time is also required. The study of disconnected charm quark loops may also be useful for looking at hidden charmonium [79].

ACKNOWLEDGMENTS

We thank Alex Dougall and Chris Maynard for discussions. The lattice data was generated on the Cray T3D and T3E systems at EPCC supported by EPSRC grant GR/K41663, PPARC grants GR/L22744 and PPA/G/S/1998/00777. We are grateful to the ULgrid project of the University of Liverpool for computer time. The authors acknowledge support from EU grant HPRN-CT-2000-00145 Hadrons/LatticeQCD.

[1] S. Stone, hep-ph/0310153.
[2] S. Bianco, F.L. Fabbri, D. Benson, and I. Bigi, Riv. Nuovo Cimento **26**, 1 (2003).
[3] HPQCD Collaboration, C.T.H. Davies *et al.*, Phys. Rev. Lett. **92**, 022001 (2004).
[4] M. Di Pierro *et al.*, Nucl. Phys. B (Proc. Suppl.) **119**, 586 (2003).
[5] UKQCD Collaboration, C.R. Allton *et al.*, Phys. Lett. B **292**, 408 (1992).
[6] A.X. El-Khadra, Nucl. Phys. B (Proc. Suppl.) **30**, 449 (1993).
[7] C.T.H. Davies *et al.*, Phys. Rev. D **52**, 6519 (1995).
[8] H.D. Trottier, Phys. Rev. D **55**, 6844 (1997).
[9] N.H. Shakespeare and H.D. Trottier, Phys. Rev. D **58**, 034502 (1998).
[10] N. Mathur, R. Lewis, and R.M. Woloshyn, Phys. Rev. D **66**, 014502 (2002).
[11] T.R. Klassen, Nucl. Phys. B (Proc. Suppl.) **73**, 918 (1999).
[12] P. Chen, Phys. Rev. D **64**, 034509 (2001).

[13] CP-PACS Collaboration, M. Okamoto *et al.*, Phys. Rev. D **65**, 094508 (2002).
[14] C. McNeile, hep-lat/0210026.
[15] QCD-TARO Collaboration, S. Choe *et al.*, Nucl. Phys. B (Proc. Suppl.) **106**, 361 (2002).
[16] QCD-TARO Collaboration, S. Choe *et al.*, J. High Energy Phys. **08**, 022 (2003).
[17] C.W. Bernard *et al.*, Phys. Rev. D **62**, 034503 (2000).
[18] A.X. El-Khadra, S. Gottlieb, A.S. Kronfeld, P.B. Mackenzie, and J.N. Simone, Nucl. Phys. B (Proc. Suppl.) **83**, 283 (2000).
[19] C. Stewart and R. Koniuk, Phys. Rev. D **63**, 054503 (2001).
[20] C.W. Bernard *et al.*, Phys. Rev. D **64**, 054506 (2001).
[21] M. di Pierro *et al.*, Nucl. Phys. B (Proc. Suppl.) **129**, 340 (2004).
[22] S. Gottlieb, Nucl. Phys. B (Proc. Suppl.) **128**, 72 (2004); **129**, 17 (2004).
[23] UKQCD Collaboration, P. Lacock and C. Michael, Phys. Rev. D **52**, 5213 (1995).
[24] G.S. Bali, hep-lat/0308015.
[25] UKQCD Collaboration, C. McNeile, C. Michael, and K.J. Sharkey, Phys. Rev. D **65**, 014508 (2002).
[26] UKQCD Collaboration, P. Boyle, Nucl. Phys. B (Proc. Suppl.) **53**, 398 (1997).
[27] UKQCD Collaboration, P. Boyle, Nucl. Phys. B (Proc. Suppl.) **63**, 314 (1998).
[28] J. Hein *et al.*, Phys. Rev. D **62**, 074503 (2000).
[29] UKQCD Collaboration, K.C. Bowler *et al.*, Nucl. Phys. **B619**, 507 (2001).
[30] UKQCD Collaboration, J.M. Flynn, F. Mescia, and A.S.B. Tariq, J. High Energy Phys. **07**, 066 (2003).
[31] Particle Data Group, K. Hagiwara *et al.*, Phys. Rev. D **66**, 010001 (2002).
[32] Y. Kuramashi, M. Fukugita, H. Mino, M. Okawa, and A. Ukawa, Phys. Rev. Lett. **72**, 3448 (1994).
[33] CP-PACS Collaboration, A. Ali Khan *et al.*, Nucl. Phys. B (Proc. Suppl.) **83**, 162 (2000).
[34] W. Bardeen, A. Duncan, E. Eichten, and H. Thacker, Phys. Rev. D **62**, 114505 (2000).
[35] SESAM Collaboration, T. Struckmann *et al.*, Phys. Rev. D **63**, 074503 (2001).
[36] UKQCD Collaboration, C. McNeile and C. Michael, Phys. Lett. B **491**, 123 (2000).
[37] W. Lee and D. Weingarten, Nucl. Phys. B (Proc. Suppl.) **63**, 194 (1998).
[38] W. Lee and D. Weingarten, Nucl. Phys. B (Proc. Suppl.) **73**, 249 (1999).
[39] W. Lee and D. Weingarten, Phys. Rev. D **61**, 014015 (2000).
[40] UKQCD Collaboration, C. McNeile and C. Michael, Phys. Rev. D **63**, 114503 (2001).
[41] UKQCD Collaboration, A. Hart, C. McNeile, and C. Michael, Nucl. Phys. B (Proc. Suppl.) **119**, 266 (2003).
[42] N. Isgur and H.B. Thacker, Phys. Rev. D **64**, 094507 (2001).
[43] UKQCD Collaboration, C.R. Allton *et al.*, hep-lat/043007.
[44] H. Neff, N. Eicker, T. Lippert, J.W. Negele, and K. Schilling, Phys. Rev. D **64**, 114509 (2001).
[45] UKQCD Collaboration, C.R. Allton *et al.*, Phys. Rev. D **65**, 054502 (2002).
[46] UKQCD Collaboration, A. Dougall, R.D. Kenway, C.M. Maynard, and C. McNeile, Phys. Lett. B **569**, 41 (2003).
[47] UKQCD Collaboration, A. Dougall, C.M. Maynard, and C. McNeile, Nucl. Phys. B (Proc. Suppl.) **129**, 170 (2004).
[48] UKQCD Collaboration, P. Lacock, A. McKerrell, C. Michael, I.M. Stopher, and P.W. Stephenson, Phys. Rev. D **51**, 6403 (1995).
[49] A.X. El-Khadra, A.S. Kronfeld, and P.B. Mackenzie, Phys. Rev. D **55**, 3933 (1997).
[50] C.W. Bernard, J.N. Labrenz, and A. Soni, Phys. Rev. D **49**, 2536 (1994).
[51] M. Luscher, S. Sint, R. Sommer, and P. Weisz, Nucl. Phys. **B478**, 365 (1996).
[52] S. Aoki, Y. Kuramashi, and S.-i. Tominaga, Prog. Theor. Phys. **109**, 383 (2003).
[53] JLQCD Collaboration, S. Aoki *et al.*, Nucl. Phys. B (Proc. Suppl.) **53**, 355 (1997).
[54] T. Skwarnicki, Int. J. Mod. Phys. A **19**, 1030 (2004).
[55] C. Edwards *et al.*, Phys. Rev. Lett. **48**, 70 (1982).
[56] A. Martin and J.M. Richard, Phys. Lett. **115B**, 323 (1982).
[57] BELLE Collaboration, S.K. Choi *et al.*, Phys. Rev. Lett. **89**, 102001 (2002).
[58] CLEO Collaboration, J. Ernst *et al.*, hep-ex/0306060.
[59] BABAR Collaboration, B. Aubert *et al.*, hep-ex/0311038.
[60] C. Thron, S.J. Dong, K.F. Liu, and H.P. Ying, Phys. Rev. D **57**, 1642 (1998).
[61] W. Wilcox, hep-lat/9911013.
[62] C.J. Morningstar and M.J. Peardon, Phys. Rev. D **60**, 034509 (1999).
[63] M. Suzuki, Phys. Rev. D **65**, 097507 (2002).
[64] T. Schafer and E.V. Shuryak, hep-lat/0005025.
[65] C. Michael, Phys. Rev. **156**, 1677 (1967).
[66] P. Geiger and N. Isgur, Phys. Rev. D **41**, 1595 (1990).
[67] N. Isgur, Phys. Rev. D **60**, 054013 (1999).
[68] K. Heikkila, S. Ono, and N.A. Tornqvist, Phys. Rev. D **29**, 110 (1984).
[69] W.A. Bardeen, A. Duncan, E. Eichten, N. Isgur, and H. Thacker, Phys. Rev. D **65**, 014509 (2002).
[70] C. McNeile, hep-lat/0307027.
[71] C. Michael, Nucl. Phys. B (Proc. Suppl.) **128**, 153 (2004).
[72] UKQCD Collaboration, C. McNeile and C. Michael, Phys. Lett. B **556**, 177 (2003).
[73] G.T. Bodwin, E. Braaten, and G.P. Lepage, Phys. Rev. D **51**, 1125 (1995); **55**, 5853(E) (1997).
[74] G.T. Bodwin and A. Petrelli, Phys. Rev. D **66**, 094011 (2002).
[75] W. Kwong, P.B. Mackenzie, R. Rosenfeld, and J.L. Rosner, Phys. Rev. D **37**, 3210 (1988).
[76] CLEO Collaboration, G. Brandenburg *et al.*, Phys. Rev. Lett. **85**, 3095 (2000).
[77] BES Collaboration, J.Z. Bai *et al.*, Phys. Lett. B **555**, 174 (2003).
[78] BABAR Collaboration, G. Wagner, hep-ex/0305083.
[79] S.J. Brodsky and S. Gardner, Phys. Rev. D **65**, 054016 (2002).